Advances in Physics Theories and Applications
ISSN 2224-719X (Paper) ISSN 2225-0638 (Online)
Vol.31, 2014
www.iiste.org

Effect of Thermal Annealing on the Structural, Optical, and Electrical Properties of a-Se Thin Films

Fuad Mutar[1] Ayser Hemed[2*]

1. Expert, Governmental of Curricula, Ministry of Education, State of Iraq, P. Address: Governmental of Curricula, Ministry of Education, Baghdad, Iraq.
2. Department of Physics, College of Education, University of Mustansiryah, Baghdad, Iraq.

P. Address: Department of Physics, College of Education, University of Mustansiryah, Baghdad, Iraq.
* E-mail of the corresponding author: ayserah@live.com

The research is financed by researchers themselves.

Abstract:

In this experimental study, Structural, electrical and optical properties of as-grown and annealed films for the amorphous Selenium was carried out. Growing for the samples was done on glass substrates by thermal evaporation technique under pressure range 10-5 - 10-6 Torr at room temperature. The structure of amorphous Selenium thin film was investigated by X-ray diffraction (XRD) for three different annealing temperatures (323, and 363K). The result of the X-ray diffraction studied at 363K indicated the formation of Selenium with Hexagonal Phase. The transmission spectra of annealed and as-deposited films have been carried out for the range UV-Visible transmittance spectrum (wavelength range of 200-1100 nm) at room temperature. Results showed that the absorption coefficient for the previous range was $\alpha \geq 10^4\,cm^{-1}$. Results for the optical band gap gave a direct one, within the energy range (2.01-2.11) eV. These experimental values of the optical band gap indicated an inversely proportionated with annealing temperature. Results for both D.C and A.C conductivity for the temperature range 295.5 to 363K showed that both type of conductivity related linearly temperature. Results showed that the A.C. conductivity increases linearly with the frequency at the range (10^2-10^5) Hz. Results for the activation energy (E_a) shows that it related linearly with the annealing temperature.

Keywords: Amorphous Selenium, Chalcogenide, X-Ray diffraction (XRD).

1. Introduction:

Selenium can be produced in three basic structures: (a) the most common and most stable phase In the last three decades, much more attention has been paid for studying the most commercial important Chalcogenide semiconductors, the amorphous selenium (a-Se) and its alloys. This fast attention given to the various allotropes of Selenium and their inter-conversion arises from its use in a variety of electronics and solid-state technological applications. Selenium exhibits both photovoltaic and photoconductive actions, thus formulating its function in the production of photocells and exposure meters for photographic use as well as solar cells. Amorphous selenium (a-Se) is also extensively utilized in rectifiers, xerography and glass industry to decolorize glass and make ruby-colored glasses and enamels.
hexagonal structure, which shows high electrical conductivity, (b) relatively high resistive semiconductor of monoclinic structure which can be synthesized by growth from chemical solution and may be transformed into the hexagonal structure by heating, and (c) the supercooled liquid amorphous structure, which may be easily obtained by rapidly cooling from the liquid phase so that crystallites do not form.

2. Experimental:

Selenium thin films was prepared by the vacuum evaporation of black Selenium (purity of: 99%) in a high vacuum (5×10-6 mbar) on a glass substrate at room temperature. The deposition process started with constant deposition rate equal to 10 Å/sec.
The corning glass substrate (Soda Lim Glass)was cleaned by using detergent with water to remove any oil or dust that might be attached to the surface of substrate and then they were placed under tap water and rubbing gently for 15 minutes. Then they were placed in a clean beaker containing distilled water and then rinsed in ultrasonic unit for 15 minutes. After that repeated it by replacing the distilled water with pure Alcohol solution which reacts with contamination such as grease and some Oxides. The sample was kept in dry place with away from air and dust particles. Thin a-Se films at room temperature with different annulling temperature (323, 343 and 363 K) were obtained. The structural characterization was carried out by taking XRD pattern of the films with the help of Philips X-Ray diffractometer using target Cu-Kα (λ=1.54060 Å) radiations as X-ray source. The current has been 30 mA and the voltage was (40 KV). The scanning angle 2θ has varied in the range of (20 – 60)

degree with speed of (4) deg/min. The interplaner distance dhkl for different planes was determined by using Bragg's law. UV-Visible transmittance spectrums of the films were measured at normal incidence in the spectral range of (200-1100nm). The electrical conductivity has been measured as a function of temperature for Se films in the range (R.T. –363) K by using the electrical circuit. The measurements have been done using sensitive digital electrometer type keithley (616) and electrical oven. For A.C. measurement, an HP-R2C unit model (4275 A) multi frequency LCR meter has been used to measure the capacitance (C) and resistance (R) with frequency range between 100Hz-100 kHz. A.C. instrument is shielded by the copper sheet to avoid the distortion signal, and to prohibit the connectors among the experimental portion from becoming a source of noise by using coaxial cables and BNC connectors are used. The amplitude of measuring ac signal has been kept low at 0.08 volt to avoid possible non linearity and instability.

3. Results and Discussion:

3-1 Structural Analysis:

The XRD results of Selenium films prepared at room temperature with different annealing temperatures (323,343 and363) K, are shown in fig.1. The XRD patterns of the Selenium films at room temperature and annealed temperature 323K shows amorphous structure of the 2θ range (20-60). On the other hand, the XRD patterns of selenium films annealed at temperature 343K shows the peaks that started to grow, and appeared in Ta=363 K which exhibit a prominent reflection angle 2θ=23.49°and 2θ=29.70°. This is due to the increase of grain size and can be explained by the movement of atoms after annealing to array its selves in different sizes of grains. The crystal lattice is hexagonal structure, it was normalized by[Keller R.].This result is agreement Champness and Pan results. Table 1, shows the 2θ and d-spacing observed along with the standard data (Crystallography Open Database (COD) No.96-901-1649 Se).

3-2 The Optical Part:

The optical properties of Se films for 500 nm thickness at different annealing temperatures have been study by UV-Visible transmittance spectrum.

The transmission spectra of annealed and as-deposited films have been illustrated in Fig 2. From these plots shows that the increasing of annealing temperature caused to shifts the peak of transmittance spectrum toward the shorter wavelengths (higher energies compared with the as-deposited film, which means the decrease in disorder and defect density in the structure gives rise to increase in the optical band gap. In addition, the saturation of dangling bonds in the amorphous structure results in increase in band gap.

3-2-1 the Absorption Coefficient:

The absorption coefficient of the Se films is characterized by strong absorption at shorter wavelengths region between (200-580) nm and without sharp edge on the long wavelength side from (600-1100) nm.

In the shorter wavelength the absorption coefficient exhibits higher values within the range (1.25-4.5)×104 cm-1, Fig. 3.

3-2-2 The Optical Energy Gap:

In the high absorption region ($\alpha \geq 10^4\,cm^{-1}$), the variation of the absorption coefficient with photon energy is obtained using the relation:

$$\alpha h\nu = B(h\nu - E_g)^r \qquad (1)$$

where h is Planck constant, ν is the frequency, B is an energy independent constant (it is a parameter which depends on the transition probability), E_g is the optical energy gap of the investigated films, and r is a number characterizing the transition process, having the values (1/2, 3/2, 2 and 3) for direct allowed, direct forbidden, indirect allowed and indirect forbidden transitions, respectively.

The E_g values are estimates from the extrapolation to zero absorption in Tauc equation(1) and lie within the range (2.01-2.11) eV, the values of E_g^{α} decrease with increasing annealing temperature that is because the width of localized states near the mobility edges depends on the degree of disorder and defects present in amorphous structure. In particular it is known that unsaturated bonds together with some saturated bonds are produced as a result of insufficient number of atoms deposited in the amorphous films. These unsaturated bonds are responsible for the formation of some defects in the films, which produce localized state in the amorphous solids.

The presence of a high concentration of localized states in the band structure has been responsible for low values of optical energy gap and electrical activation energy in both as-prepared amorphous films and those annealed, fig. 4. This result is in agreement with K. S. Bindra et.al. in 2006 [8].

On the basis of experimental results, it is concluded that band gap of thin films is also thickness dependent. It is

observed that the band gap of the thin films increases with increasing the thickness of the films. Figs. 5 and 6 shows the variation of the band gap of the film with the increase in film thickness and it increases for the thickness in the (300,500 and 700) nm. The estimated values of the band gaps are similar to the value reported by Khan et.al. in 2010.

It may be mentioned that, in amorphous Chalcogenide thin films, the number of defects are higher due to the existence of unsaturated bonds. The increase in the thickness of the films results in a homogeneous network with low density of defects thereby, increasing the optical band gap.

3-3: The Electrical Part:

3.3.1. D.C. Conductivity:

In order to study conductivity mechanisms, it is convenient to plot logarithm of the conductivity ($\ln\sigma$) as a function of $1000/T$ for a-Se films with different annealing temperatures. It is found that the conductivity of all samples increases with the increase in temperature from (295.5 to 363) K. This result agrees with Khan in 2010.

Fig.7 shows the temperature dependence of D.C. conductivity in the amorphous selenium thin films in the temperature range (295.5- 363) K for all the samples. The plots ($\ln \sigma_{dc}$) versus ($1000/T$) are found to be straight lines in the temperature range of (314–363) K indicating that the conduction in these samples is through an thermally activated process. Conductivity varies in accordance with the equation:

$$\sigma = \sigma_o \exp(-E_a/kBT) \qquad (2)$$

where: σ_o is the minimum electrical conductivity, E_a is the activation energy, T is temperature and, K_B is the Boltzmann constant.

One can suggest that the conduction is due to thermally assisted tunneling of charge carriers in the localized states present in the band tails.

The activation energy alone cannot decide whether the conduction is occurring in the extended states or in the band tails; because these conduction mechanisms can occur simultaneously. The activation energy in the former case represents the energy difference between mobility edge and the Fermi level, $(E_c - E_F)$ or $(E_F - E_V)$; while in the letter case it represents the sum of the energy separation between the occupied localized states and the Fermi level $(E_F - E_V)$, and the mobility activation energy for the hopping process between the localized states.

In the low temperature range (295.5 – 314) K, the conductivity increases very slowly with temperature, this implies that the conduction occurs via variable range hopping of the charge carriers in the localized states near the Fermi level. This result agrees with the study of Majeed Khan in 2010. Table 2 shows an increase in the activation energy (E_a) values with the increase of T_a.

3.3.2. A.C. Conductivity:

The dependence of A.C. conductivity $\sigma_{A.C}$ of the layer system of Al/Se/Al sample on frequency with the frequency range (10^2 -10^5) Hz at different annealing temperatures will be report as the following:

3.3.2.1. A.C. Conductivity Dependence on Frequency:

The variation of A.C. conductivity with the frequency for Se films at R.T. and different annealing temperature (323, 343 and 363) K have been shown in fig.8. The A.C. conductivity increases with the increasing frequency for all samples. $\sigma_{a.c}(\omega)$ is proportional to ωs which means that $\sigma_{a.c}(\omega)$ dominates at higher frequency, in the range of (10^3 – 10^5) Hz. For lower frequency in the range of (10^2 – 10^3) Hz $\sigma_{a.c}(\omega)$ becomes independent on the frequency because D.C. conductivity dominates in this frequency range. The values of exponent (s) are estimated from the slope of the curves plotted between $\mathrm{Ln}\sigma_{a.c}(\omega)$ versus $\mathrm{Ln}\ (\omega)$ listed in table 3.

The behavior of $s_{a.c}(\omega)$ with frequency can be explained in terms of polarization effect and hopping *i.e.* polarization effect in low frequency region where polarization is slightly changed and $s_{d.c}$ is dominated and at higher frequency region the hopping takes place. That means the exponent (s) fits C.B.H. model given by Elliott, from which A.C conductivity occurs between two sites over the barrier separating between D^+ and D^- defect centers in the band gap. This leads to greater loss in the dielectric and $s_{a.c}(\omega)$ is dominating.

3.3.2.2. A.C. Conductivity Dependence on Temperature:

The variation of lnσ(ω) as a function of the temperature (103 /T) for Se films at (3243,343 and 363) K annealing temperatures for four frequencies (10^2-10^5) Hz respectively is shown in Fig. 9 . A linear behavior of $\ln\sigma_{a.c}\ (\omega)$ of two stages has been observed over the entire temperature range (300 – 363) K indicating a thermal activated conduction mechanism. There is an activation energy for each film less than the activation energy in the D.C. conductivity because the dependences of A.C conductivity on the temperature being less than in the D.C.

conductivity. Both the A.C. activation energy $E_{\omega 1}$ and $E_{\omega 2}$ decreases as the film thickness increases as shown in table 4 and this may be attributed to increase of the absorption and decreasing the energy gap. It can be seen also that $E_{\omega 1}$ and $E_{\omega 2}$ increases with the increasing of T_a. It is obvious that there is a decrease in E_ω with frequency increasing and such result complies with the theory of CBH model.

4. Conclusions:

The structure of the nature of the Se is amorphous that a change to polycrystalline after annealing process and the crystal lattice is hexagonal. The optical transitions in Se film are direct, the absorbance of Se film for incident with an increased radiation wavelength in the range 200-600nm decreases with the increasing annealing temperate in contrast to transmittance, while for longer wavelength λ>600nm, a non-systematic change is observed.

The D.C conductivity for all films decreases with the increasing annealing temperatures. The factor(s) of the A.C conductivity decreases with the increasing of annealing temperatures. The experimental results for the mechanism of A.C conductivity are consistent with CBH model. There are two transport mechanisms of the charge carriers over the range of 295.5-363K. In general, the activation energies increase with the increasing of the annealing temperatures.

References

Solieman, A. & Abu-Sehly, A. A. (2010). Modelling of optical properties of amorphous selenium thin films. Elsevier, Physica B: Condensed Matter. 405, 4, 1101–1107. doi: http://www.sciencedirect.com/science/article/pii/S0921452609013544.

Kotkata, M.F. & Mansour, Sh. A. (2010). Current transport mechanisms for heterojunctions of a-Se on various crystalline wafers (n-Si, p-Si and n-GaAs). Elsevier, 518, 12, 3407–3412. doi: http://www.sciencedirect.com/science/article/pii/S0040609009018422.

Shaban, S. M, Saleh, R. M. & Ahmed, A. S. (2011). Characteristics $Cd_{0.3}$ $Sn_{0.7}$ Se thin films as absorber materials for Solar cell devices. Turkish J. Phys. 35, 189 –196. doi: doi:10.3906/fiz-0909-8.

Keller, R., Holzapfel, W. B. & Schulz, H. (1977). Effect of pressure on the tom positions in Se and Te Locality: synthetic Note: known as alpha has with trigonal structure, Physical Review, 16, 4404-4412.

Champness, C. H. & Pan, J. (1988). Anomalous behavior in the capacitance of selenium Schottky diodes, Canadian Journal of Physics. 66, 2, 168-174. Doi: 10.1139/p88-025.

Karaagac, H. (2010). Electrical, structural and optical preparation of AgGaSe $_{2\text{-}X}$ S_X thin films grown by sintered powder. A Ph.D. thesis submitted to the graduate shool of natural and applied sciences of Middle East technical University. doi: http://etd.lib.metu.edu.tr/upload/12612362/index.pdf

Mott, N. F. & Davis, E. A. (2012). Electronic Processes in Non-Crystalline Materials. Oxford Classic Texts in the Physical Sciences, Clarendon Press, 2nd edition, Oxford, UK. doi: http://ukcatalogue.oup.com/product/9780199645336.do

Bindra, K. S., Suri N. & Thangaraj R. (2006). Effect of annealing on the structure and optical proprieties of a-Se-Sb-Ag thin films. Chalcogenide Letters. 3, 9,133 – 138. doi: http://www.chalcogen.ro/Bindra-Nikhil.pdf

Khan, Z. R., Zulfequar, M. & Khan, S. (2010). Effect of thickness on structural and optical proprieties of thermal evaporation polycrystal thin, Chalcogenide Letters, 7, 6, 431- 438. doi: http://www.chalcogen.ro/431_Raza-Khan.pdf.

Sati, D.C., Kumar, R. & Mehra R. M. (2006). Influence of thickness on optical properties of a:As_2Se_3 thin films. Turkish J. Phys. 30, 519 – 527. doi: http://journals.tubitak.gov.tr/physics/issues/fiz-06-30-6/fiz-30-6-6-0608-3.pdf.

Khan, Z. H., Khan S. A., Salah, N., Habib, S., El-Hamidy, S. M. A. & Al-Ghamdi A. A. (2010). Effect of composition on electrical and optical properties of thin films of amorphous Ga_xSe_{100-2x} Nanorods. Nanoscale Res. Lett. 5, 1512–1517. doi: 10.1007/s11671-010-9671-5.

Khan, M. A. M., Kumar, S., Khan M. W., Husain M. & Zulfequar M. (2010). Electrical transport mechanisms in a-Se95M5 films (M=Ga, Sb, Bi). Materials Research Bulletin. 45, 6, 727-732. doi: http://www.sciencedirect.com/science/article/pii/S0025540810000607.

Elliott, S. R. (1987). A.C. Conduction in amorphous chalcogenide and pnictide semiconductors. Advance in physics. An e-book published by Taylor & Francis Group. 36. 2. 135-217. doi: 10.1080/00018738700101971.

Tables and Figures:

Table 1. X-Ray diffraction data for Se thin film prepared at 363K, comparative with standard data.

2θ[degree] Exp.	dhkl [Å] Exp.	I/I_o% Exp.	dhkl [Å] Std.	I/I_0% Std.	hkl Std.
23.49	3.7842	40.42	3.7828	44	100
29.70	3.0056	33.68	3.007	100	101
43.68	2.0706	10.26	2.0734	32	102
51.92	1.7597	6.66	1.7672	21	201
55.93	1.6427	5.34	1.6527	6	003

Amorphous structure of the 2θ and d-spacing observed experimentally in compared with the standard data) Crystallography Open Database (COD) (No.96-901-1649 Se).

Table 2. D.C. Conductivity parameters for a-Se films at different annealing temperatures for (500nm) thickness.

$T_a(K)$	(295.5-314)K $E_{a1}(eV)$	(314–363) K $E_{a2}(eV)$	$\sigma_{R.T} \times 10^{-8}$ $(\Omega.cm)^{-1}$
R.T.	0.26	0.31	14.32
323	0.27	0.32	1.44
343	0.29	0.38	1.39
363	0.34	0.44	1.34

The increase in activation energy (E_a) values with the increase of T_a.

Table 3. Exponent (S) value of a-Se films at different annealing temperatures for (500nm) thickness.

T_a(K)	R.T.	323	343	363
S	0.967	0.935	0.867	0.711

Decrease of exponent (S) value of a-Se films with annealing temperatures for (500nm) thickness.

Table 4. A.C Activation energies for Se films at annealing temperatures with (100, 1000, 10000 and 100000) Hz.

T_a(K)	$E_{\omega1}(eV)$				$E_{\omega2}(eV)$			
	Frequency (Hz)							
	10^2	10^3	10^4	10^5	10^2	10^3	10^4	10^5
R.T.	0.0753	0.0487	0.0398	0.0099	0.0598	0.0433	0.0269	0.0161
323	0.0922	0.0878	0.0526	0.0013	0.1161	0.0201	0.0123	0.0174
343	0.0952	0.0788	0.0631	0.0092	0.2128	0.1293	0.0499	0.0317
363	0.1248	0.1141	0.1022	0.0126	0.2117	0.1818	0.1106	0.0634

The A.C activation energy $E_{\omega1}$ and $E_{\omega2}$ for films decreased as the thickness increased.

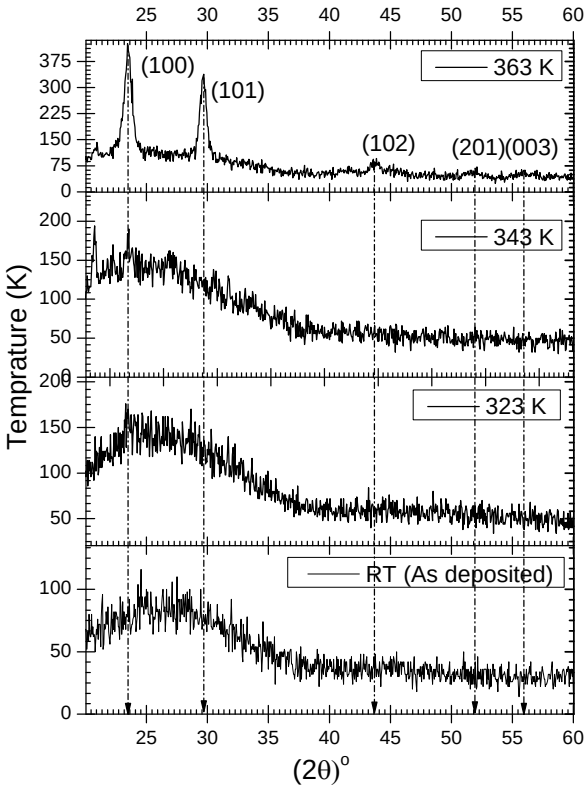

Figure 1. XRD of Se with different annealing temperatures.

Peaks started to grow prominent, reflection angel from 2θ=23.49°, due to the increase of grain size.

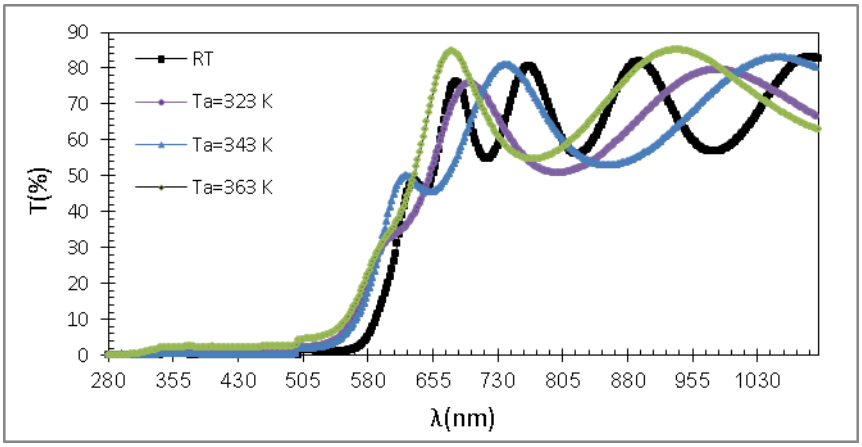

Figure 2. The transmittance spectrum at different annealing temperature for 500nm a-Se thin films.

The increasing of annealing temperature caused to shifts the peak of transmittance spectrum toward the shorter wavelengths.

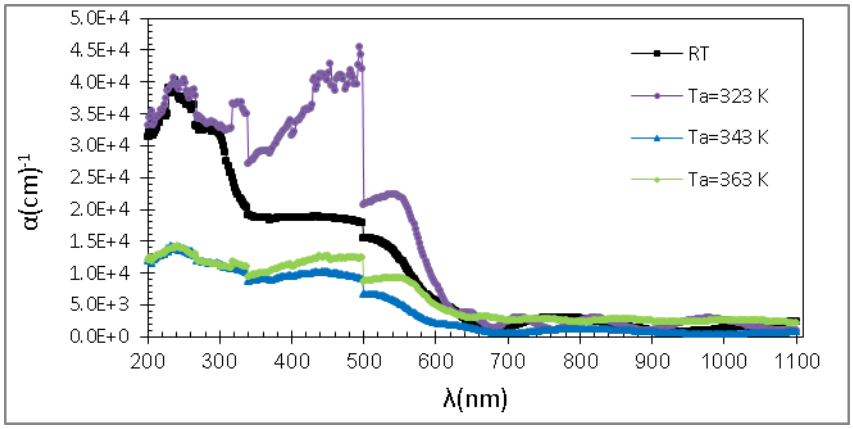

Figure 3. The absorption coefficient at different annealing temperature for (500nm) thickness of Se thin films.

The absorption coefficient of the Se films is characterized by strong absorption at shorter wavelengths region between (200-580) nm and without sharp edge on the long wavelength side from (600-1100) nm.

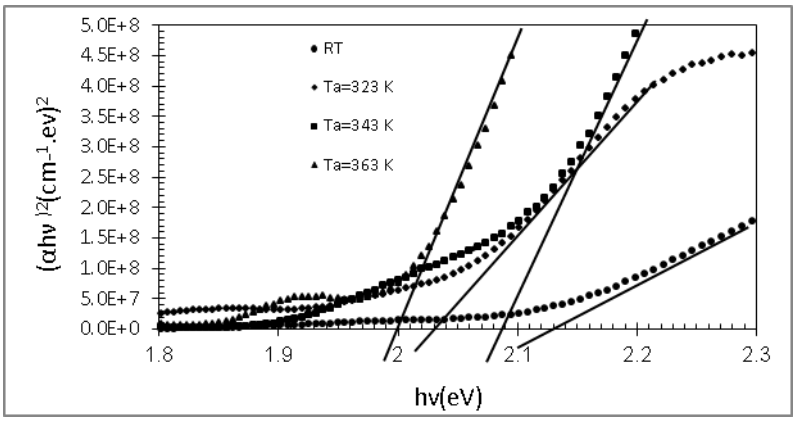

Figure 4. The absorption coefficient plotted as (αhν)2 versus hν at different annealing temperature of a-Se thin films for (500nm) thickness.

The presence of a high concentration of localized states in the band structure has been responsible for low values of optical energy gap and electrical activation energy in both as-prepared amorphous films and those annealed.

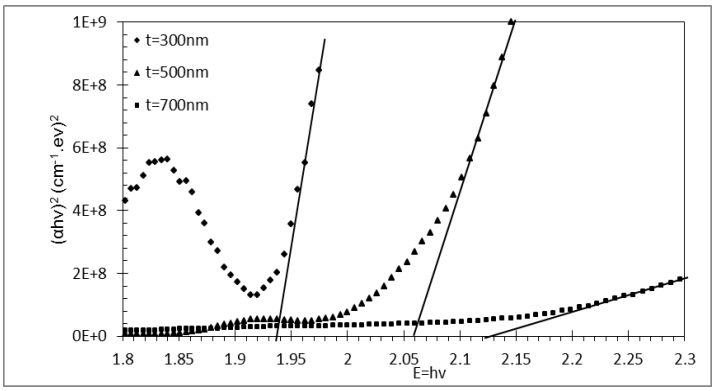

Figure 5. The absorption coefficient plotted as (αhν)2 versus hν of a-Se thin films with different thickness at annealing temperature (323)K.

It is observed that the band gap of the thin films increases with increasing the thickness of the films.

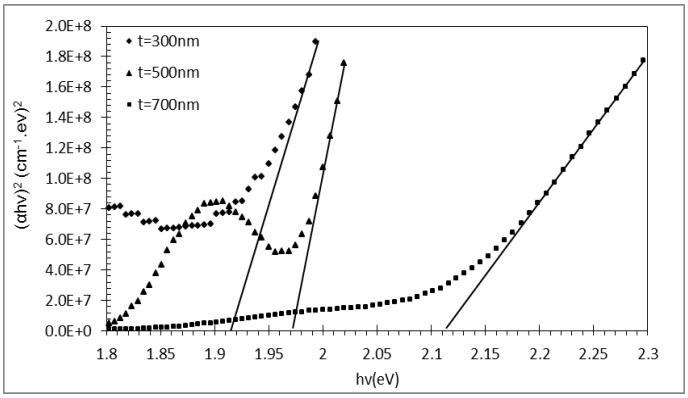

Figure 6. The absorption coefficient plotted as $(\alpha h\nu)2$ versus $h\nu$ of a-Se thin films with different thickness at annealing temperature (343)K.

It is observed that the band gap of the thin films increases with increasing the thickness of the films.

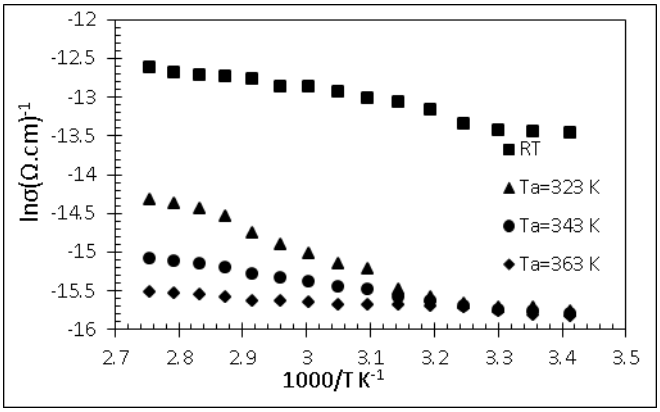

Figure 7. Ln σ versus 1000/T for a-Se films at thickness 500nm and different annealing temperatures.

The plots $(\ln \sigma_{dc})$ versus $(1000/T)$ are found to be straight lines in the temperature range of (314–363) K indicating that the conduction in these samples is through an thermally activated process.

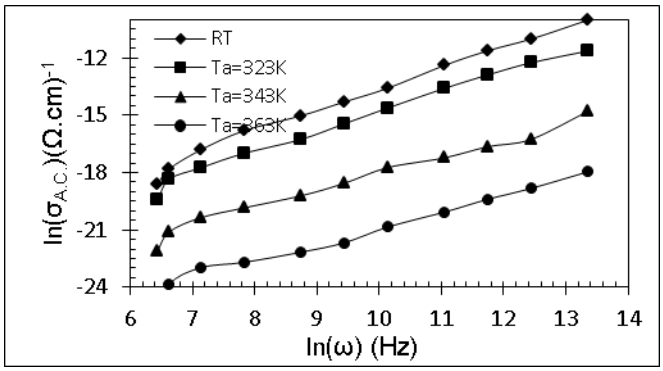

Figure 8. $Ln\sigma_{a.c}$ as a function of Ln(ω) for a-Se films at different annealing temperatures for (500nm) thickness.

The A.C. conductivity increases with the increasing frequency for all samples. $\sigma_{a.c}(\omega)$ is proportional to ωs which means that $\sigma_{a.c}(\omega)$ dominates at higher frequency, in the range of (10^3 – 10^5) Hz.

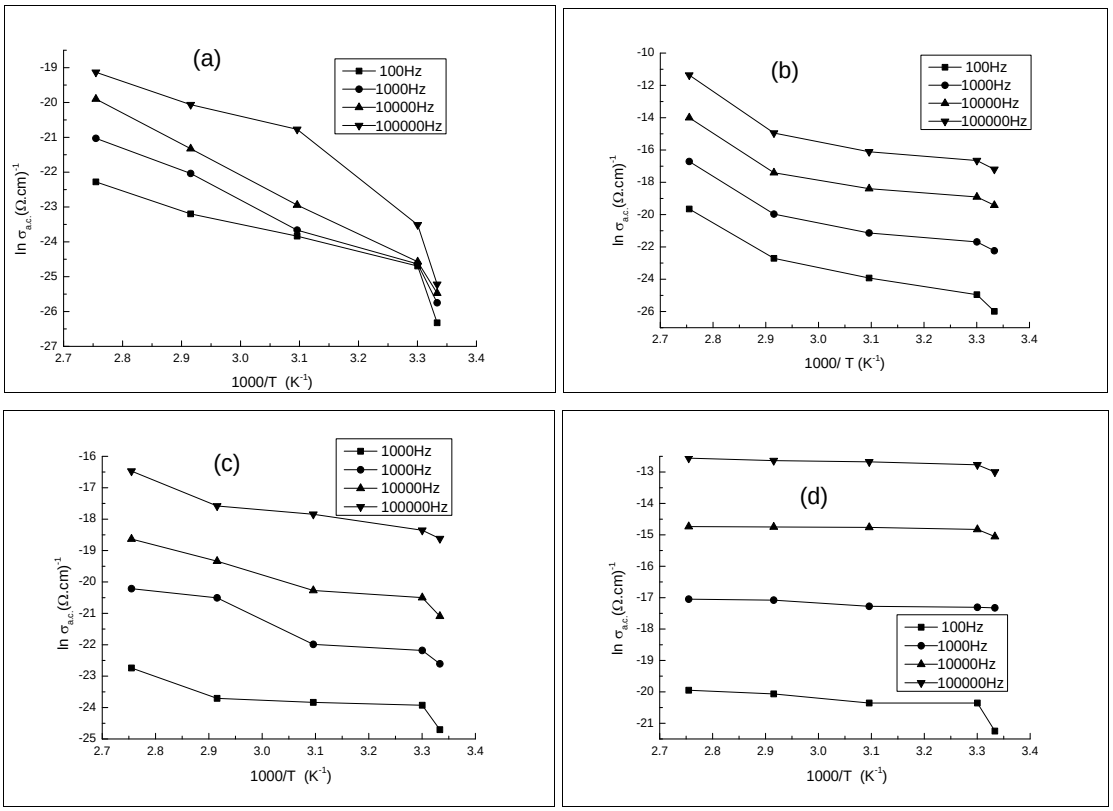

Figure 9. Ln $\sigma_{a.c}$ as a function of 1000/T for a-Se films with thickness 500nm and at annealing temperatures (a) 303K (b) 323K (c) 343K & (d) 363K.

A linear behavior of $\ln\sigma_{a.c}\ (\omega)$ of two stages has been observed over the entire temperature range (300 – 363) K indicating a thermal activated conduction mechanism.

The IISTE is a pioneer in the Open-Access hosting service and academic event management. The aim of the firm is Accelerating Global Knowledge Sharing.

More information about the firm can be found on the homepage:
http://www.iiste.org

CALL FOR JOURNAL PAPERS

There are more than 30 peer-reviewed academic journals hosted under the hosting platform.

Prospective authors of journals can find the submission instruction on the following page: http://www.iiste.org/journals/ All the journals articles are available online to the readers all over the world without financial, legal, or technical barriers other than those inseparable from gaining access to the internet itself. Paper version of the journals is also available upon request of readers and authors.

MORE RESOURCES

Book publication information: http://www.iiste.org/book/

Recent conferences: http://www.iiste.org/conference/

IISTE Knowledge Sharing Partners

EBSCO, Index Copernicus, Ulrich's Periodicals Directory, JournalTOCS, PKP Open Archives Harvester, Bielefeld Academic Search Engine, Elektronische Zeitschriftenbibliothek EZB, Open J-Gate, OCLC WorldCat, Universe Digtial Library , NewJour, Google Scholar